ACS Macro Letters

Letter

Cite This: ACS Macro Lett. 2019, 8, 228−232

pubs.acs.org/macroletters

Polyethylene Grafted Silica Nanoparticles Prepared via Surface-Initiated ROMP

Julia Pribyl,[†] Brian Benicewicz,*[,†] Michael Bell,[‡] Kenneth Wagener,[‡] Xin Ning,[§] Linda Schadler,[∥] Andrew Jimenez,[⊥] and Sanat Kumar[⊥]

[†]Department of Chemistry and Biochemistry, University of South Carolina, Columbia, South Carolina 29208, United States

[‡]The George and Josephine Butler Polymer Research Laboratory, Department of Chemistry, University of Florida, Gainesville, Florida 32601, United States

[§]Department of Materials Science and Engineering, Rensselaer Polytechnic Institute, Troy, New York 12180, United States

[∥]Department of Engineering and Mathematical Sciences, University of Vermont, Burlington, Vermont 05405, United States

[⊥]Department of Chemical Engineering, Columbia University, New York, New York 10027, United States

Supporting Information

ABSTRACT: Polyethylene and nanosilica represent the most ubiquitous commodity plastic and nanocomposite filler, respectively. Despite their potential utility, few examples exist in the literature of successfully combining these two materials to form polyethylene nanocomposites. Synthesizing well-defined polyethylene grafted to a surface is a significant challenge in the nanocomposites community. Presented here is a synthetic approach toward polyethylene grafted nanoparticles with controllable graft density and molecular weight of the grafted polymer. The variably grafted nanoparticles were then incorporated into a commercial high density polyethylene matrix. The synthesis, characterization, and challenges in making these materials are discussed.

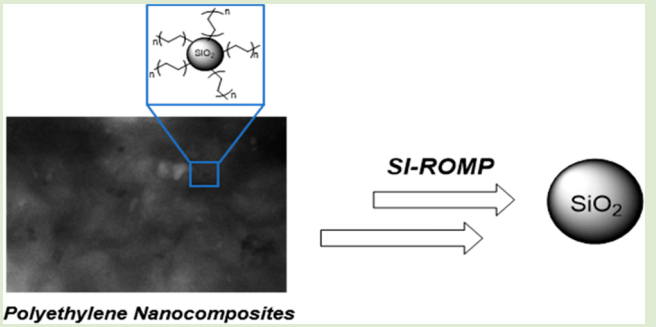

Polyolefin materials represent the largest class of commodity thermoplastics in the world, and they find use in every aspect of daily life.[1] The largest subclass of commodity polyolefins, polyethylenes (PE), are abundantly used in applications from packaging to artificial joints.[2] PE is the material of choice in a variety of applications which demand chemical inertness, high strength, low density, ductility, etc., and many different classes of PE (e.g., low density PE, high density PE, linear low density PE) are synthesized commercially for different applications. PE is also a semicrystalline polymer with notably high degrees of crystallinity that provide high levels of strength and stiffness above the glass transition temperature.[3]

Despite the commercial relevance and excellent properties of PE, there are few examples of polyethylene nanocomposites stemming from the synthetic barriers involved in grafting PE on a nanosurface. Commercially, polyethylene is produced by reacting ethylene gas with a Ziegler−Natta catalyst comprised of a transition metal complex (commonly titanium or zirconium) in combination with an organoalumnium cocatalyst (e.g., triethylaluminum).[4−6] The chain growth polymerization occurs through olefin insertion between the metal center and a coordinated alkyl group. These polymerizations generally result in polymers with a broad molecular weight distribution but can also produce polyolefins with excellent stereochemical fidelity (e.g., isotactic polypropylene).[7,8] Fundamental investigation of nanocomposites has shown that control of chain graft density and molecular weight is essential for obtaining predictable nanofiller dispersion within a polymer matrix and for realizing the subsequent property enhancements.[9−11]

Polyethylene/palygorskite nanocomposites with improved impact and tensile strengths were prepared by in situ coordination polymerization, and the resulting micrometer-length palygorskite whiskers could be dispersed in a polyethylene matrix.[12] Polyethylene/nanoclay composites were prepared in a similar fashion and demonstrated improved thermal stability compared to unfilled polyethylene.[13] Nanoclays modified with a three component mixture of oligomers (styrene, lauryl acrylate, and vinyl benzyl chloride) were dispersed in both polyethylene and polypropylene and exhibited improvements in the peak heat release rate (a measure of thermal stability).[14] Dispersion of montmorillonite clays was achieved by anchoring an early transition metal complex (Ni) on the surface of the Lewis acidic clay surface, which also activates the catalyst for the in situ coordination polymerization of ethylene.[15] Additional examples of poly-

Received: December 7, 2018
Accepted: February 7, 2019

Downloaded via UNIV OF SOUTH CAROLINA COLUMBIA on February 12, 2019 at 14:30:31 (UTC).
See https://pubs.acs.org/sharingguidelines for options on how to legitimately share published articles.

© XXXX American Chemical Society

DOI: 10.1021/acsmacrolett.8b00956
ACS Macro Lett. 2019, 8, 228−232

Scheme 1. Synthetic Approach toward Nanosilica Grafted with Well-Defined Polyethylene (THF = Tetrahydrofuran, BHT = Butylated Hydroxytoluene, *p*-TSH = *para*-Toluene Sulfonyl Hydrazide, TPA= Tripropylamine; 1, Silica Nanoparticles; 2, Norbornene Grafted Nanoparticles; 3, Grubbs Catalyst Grafted Nanoparticles; 4, Polyoctene Grafted Nanoparticles; 5, Polyethylene Grafted Nanoparticles)

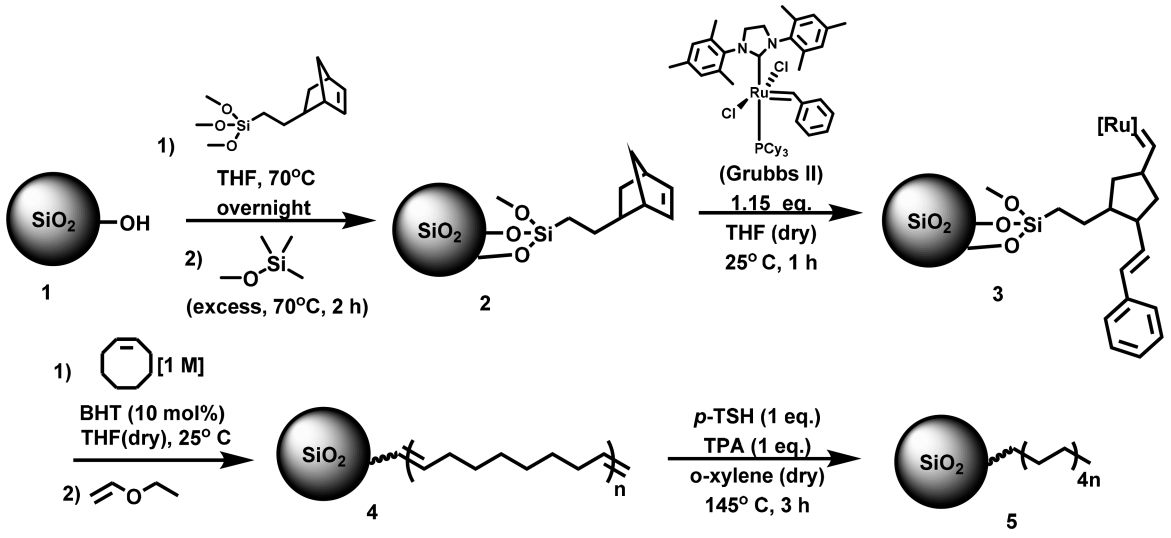

Table 1. Physical and Chemical Characteristics of Synthesized PCO-*g*-SiO_2

entry	M_n (kDa)	calcd average graft density (σ, chains/nm^2)[a]	Đ[b]	norbornyl silane feed ratio (mmol/g)	char yield before hydrogenation (%)	char yield after hydrogenation (%)	avg diameter (nm)[c,d]	T_m (°C)[e]
A	12	0.27	1.6	0.21	40.2	39.8	85	127
B	50	0.24	1.3	0.21	8.7	3.1	110	113
C	101	0.19	1.7	0.21	2.4	1.7	166	94
D	10	0.6	1.5	0.42	11.1	9.1	120	106
E	49	0.40	1.8	0.42	2.0	1.4	141	124

[a]Average graft density calculated based on the MW of grafted polymer and char yield before hydrogenation, assuming 0.15 equiv of free polymer due to excess added catalyst compared to surface-tethered norbornyl groups. [b]M_w/M_n. [c]Number-average diameter of PCO-*g*-SiO_2 determined by dynamic light scattering (DLS). [d]Diameter of Nb-*g*-SiO_2 was 16 nm as-synthesized. [e]Observed melting point on second heating after hydrogenation determined by differential scanning calorimetry (DSC).

olefin/clay composites[16,17] and polyolefin composites with carbon-based fillers also exist.[18−20]

Silica nanoparticles are of interest in the nanocomposites community because nanosilica is easy to synthesize or cheaply available commercially and has been extensively studied as a filler in amorphous materials.[21−23] Varying synthetic approaches have been used to make silica/polyolefin nanocomposites, however, achieving good dispersion of small silica nanoparticles (<50 nm) in polyolefin matrices remains a challenge.[24−28] This is largely due to the fact that few synthetic routes allow for independent control of graft density and molecular weight of the grafted chains.

Providing further motivation for well dispersed nanofillers in a popularly used semicrystalline polymer, recent work leveraged the semicrystallinity of poly(ethylene oxide) (PEO) to template the assembly of poly(methyl methacrylate) grafted silica nanoparticles (PMMA-*g*-SiO_2).[29] A 2-fold increase in the Young's modulus was observed for the ordered composite compared to the randomly dispersed composite at the same filler loading. The increased modulus was attributed to the nanoscale "brick and mortar" structure formed during crystallization. This work has exciting implications for semicrystalline polyolefin materials, especially HDPE, which has robust properties even without nanofillers. To harness this behavior in semicrystalline materials, good particle dispersion in the matrix is necessary. In this work, we present a surface-initiated ring opening metathesis polymerization (SI-ROMP) strategy to prepare linear polyethylene-grafted silica nanoparticles (PE-*g*-SiO_2); the subsequent dispersion of these nanomaterials in a high density polyethylene (HDPE) matrix will be discussed.

A strategy to synthesize linear polyethylene grafted on silica nanoparticles is detailed in Scheme 1. To begin, silica nanoparticles (**1**) were modified with a norbornyl silane at varying feed ratios as well as an alkylsilane to cap any unreacted silanol groups (**2**). This norbornyl group was then used to tether Grubbs' second-generation ruthenium catalyst to the silica nanoparticles (**3**). Many methods of catalyst attachment to surfaces have been explored in the literature, some similar to the approach described herein.[30−34] The benefit of using a norbornyl group rather than a simple alkene group is that the relief of ring strain after the catalyst reacts with the norbornene moiety generates an essentially irreversible tether compared to an alkene exchange with the catalyst's benzylidene ligand. Also, varying the feed ratio of the norbornyl silane allows for various grafted brush densities. Subsequent addition of the monomer solution to the catalyst-tethered particles resulted in grafted polycyclooctene (PCO-*g*-SiO_2, **4**). After a mild hydrogenation, the grafted polymer was transformed into linear polyethylene (**5**). A series of samples was made according to this procedure, and the physical and chemical data for these samples is shown in Table 1.

DOI: 10.1021/acsmacrolett.8b00956
ACS Macro Lett. 2019, 8, 228−232

A benefit of the described approach is that the graft density and molecular weight of the grafted polymer are independently tunable as seen in Table 1. The graft density of the polymer was qualitatively controlled by the feed ratio of norbornyl silane, and varying molecular weights of the grafted polymer were prepared by varying the monomer feed ratio. For the purposes of calculating graft densities, it was assumed that all surface-grafted norbornyl groups are initiated by the catalyst. In this case, a second-generation Grubbs catalyst was chosen because of its relative stability toward trace water and oxygen compared to a Grubbs first-generation catalyst, and it is commercially available. Obtained molecular weights agree fairly well with predicted molecular weights (indicative of high initiator efficiency), although dispersities were broad (see Supporting Information (SI) for formulation information). Similar to literature reports,[35] we observed rapid and quantitative monomer conversion by ^{1}H NMR based on the disappearance of the monomer chemical shift at 5.6 ppm and the appearance of a peak at 5.3 ppm, indicating polymer formation (SI, Figure S1). This rapid monomer conversion was observed for polymerizations both in solution and for the surface-initiated polymerization. After hydrogenation to form the PE-*g*-SiO_2 (**5**), a small decrease in the char yield was observed due to the increased saturation of the polymer backbone (SI, Figure S2). In general, the decomposition temperature was slightly higher for the unsaturated samples.

A challenge to this synthetic approach was the issue of significant particle coupling when a substoichiometric amount of catalyst was added with respect to the norbornyl silane. Figure 1 shows PCO-*g*-SiO_2 nanoparticles drop cast onto a TEM grid which were made from different catalyst ratios with respect to the amount of norbornyl silane as well as the corresponding DLS curves for the PCO-*g*-SiO_2 as synthesized. ROMP is relatively unencumbered by steric hindrance and is often used as a technique to polymerize bulky monomers.[36] It is possible for particles to irreversibly couple during this step of the synthesis if a catalyst tethered to one particle reacts with a tethered norbornyl group on another particle. It was found that using an excess of catalyst with respect to the norbornyl silane, as well as slowly adding the Nb-*g*-SiO_2 particles to a solution of catalyst, were both helpful measures in reducing particle coupling and resulted in predominantly singly dispersed polymer-grafted particles, although some small particle aggregates were still present. The hydrodynamic diameter of the polymer grafted nanoparticles measured by DLS increased substantially for each sample compared to the unmodified nanoparticles. Although the particle coupling was found to be reduced by controlling the catalyst ratio, the measured increase in hydrodynamic radius was due to both the grafted polymer and small aggregates. These results agree fairly well with the particle size and dispersion state observed by TEM.

The final step of the described synthesis is arguably the most important in preparing the PCO-*g*-SiO_2 nanoparticles for mixing with high density polyethylene (HDPE). HDPE is completely linear (i.e., contains no alkyl branches along the polymer backbone) and has a very high melting point (134 °C) because of the high degree of chain packing which occurs in the crystalline regions of the polymer. To qualitatively understand the degree of hydrogenation of the PCO-*g*-SiO_2 (termed PE-*g*-SiO_2 after hydrogenation), differential scanning calorimetry (DSC) was used to compare the thermal properties of the polymer grafted particles before and after the hydrogenation step (SI, Figure S3). After the hydrogenation, melting points ranging from 94 to 127 °C were observed during the second heating cycle, where a higher melting point indicates a higher degree of hydrogenation. Prepared samples may not reach the maximum melting temperature of HDPE because of defects in the overall crystallinity caused by the filler or incomplete saturation of the polymer.

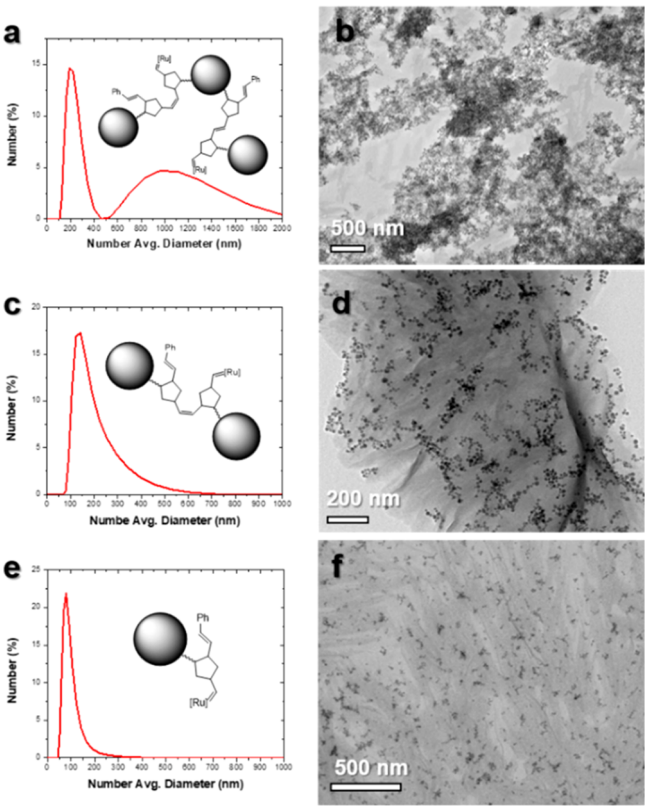

Figure 1. DLS curves and corresponding transmission electron microscopy (TEM) images of PCO-*g*-SiO_2 synthesized with (a,b) 0.8 equiv of catalyst with respect to norbornyl silane, (c,d) 1.0 equiv of catalyst with respect to norbornyl silane, and (e,f) 1.15 equiv of catalyst with respect to norbornyl silane (figures illustrate the likely coupling chemistry, but the DLS curves and TEM images are taken postpolymerization).

The dispersion states of the PE-*g*-SiO_2 particles were first observed prior to mixing with a matrix (Figure 2a,b). Qualitatively, there were still many singly dispersed particles accompanied by small aggregates, similar to the matrix-free dispersion state observed before the hydrogenation (Figure 1f). This suggests that the polymer remained grafted to the nanoparticles after hydrogenation and that the dispersion was not negatively affected by the hydrogenation procedure. The PE-*g*-SiO_2 particles were then mixed with a commercially supplied HDPE matrix (M_n = 152 kDa). The 101 kDa PE-*g*-SiO_2 showed reasonably good dispersion in the HDPE matrix with many singly dispersed particles present. Because the dispersion of single particles was observed, it is likely that the small observed aggregates were coupled prior to nanocomposite processing rather than resulting from poor wetting with the matrix polymer. Additional nanocomposite TEM images are shown in SI, Figure S4.

In this work, SI-ROMP was used to prepare PE-*g*-SiO_2 and samples with varying graft densities and MWs were prepared. A challenge inherent to this approach was the irreversible

DOI: 10.1021/acsmacrolett.8b00956
ACS Macro Lett. 2019, 8, 228−232

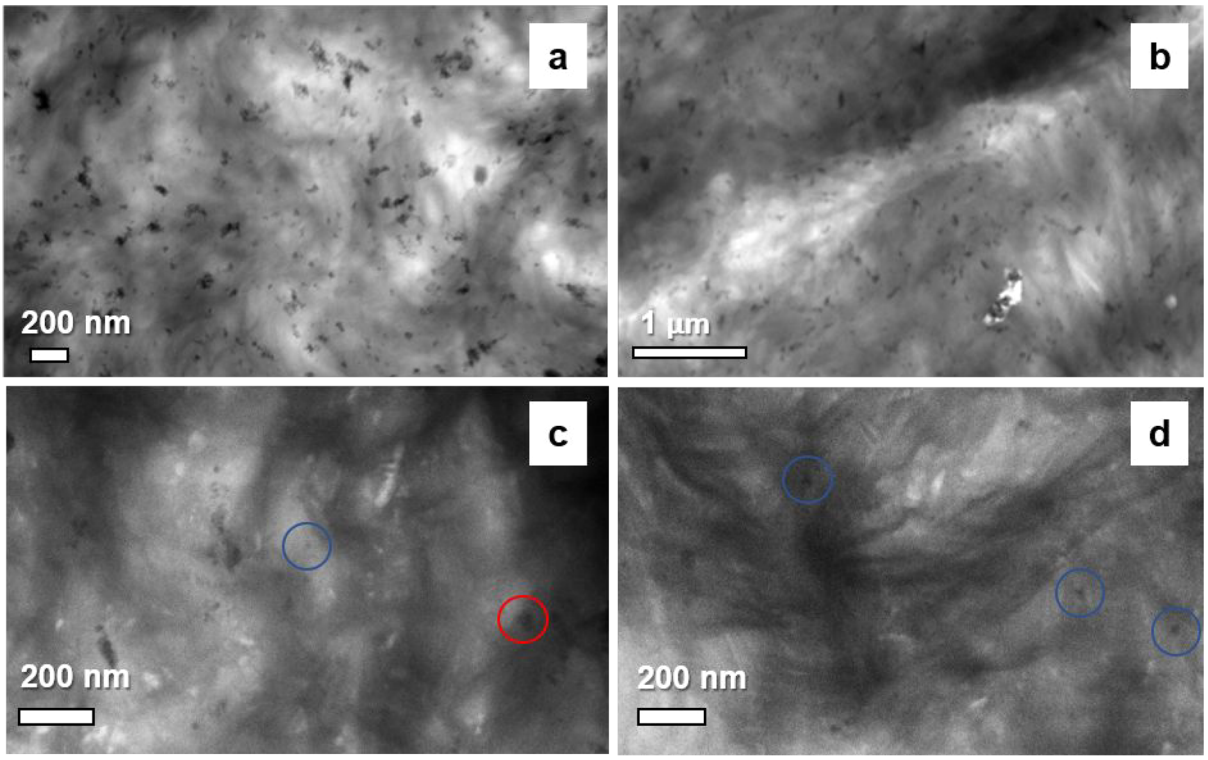

Figure 2. TEM images of (a,b) matrix free PE-*g*-SiO_2 (sample E after hydrogenation); (c,d) PE-*g*-SiO_2 (M_n = 101 kDa, σ = 0.19 chains/nm^2) dispersion in a commercial HDPE matrix, 0.6 wt % silica (matrix M_n = 152 kDa, T_m = 130 °C). For ease of viewing, some singly dispersed particles in the nanocomposite are circled in blue, and a small aggregate is circled in red for comparison.

coupling of the silica nanoparticles when a substoichiometric amount of catalyst was added, which was addressed by adding a small excess of catalyst with respect to surface-tethered norbornyl groups. A mild hydrogenation of the PCO-*g*-SiO_2 particles gave rise to PE-*g*-SiO_2. Qualitatively, the dispersion state of the particles did not change after the hydrogenation, indicating that the procedure did not have a detrimental effect on the grafted polymer or particle dispersion. The PE-*g*-SiO_2 particles were mixed with a commercial HDPE matrix, and the dispersion was observed by TEM. Many singly dispersed particles were observed in the nanocomposite, although some small aggregates existed (likely coupled prior to the nanocomposite processing). These results suggest that this synthetic approach is useful for preparing well-defined polyethylene grafted nanoparticles which are tunable in nature. In the future, this approach could be applied to many different types of nanoparticles and other polymers which are accessible by ROMP. Also, using a fast-initiating catalyst (such as Grubbs' third-generation catalyst) could potentially improve the particle coupling challenge.

■ ASSOCIATED CONTENT

Supporting Information

The Supporting Information is available free of charge on the ACS Publications website at DOI: 10.1021/acsmacrolett.8b00956.

Experimental details and supporting figures (PDF)

■ AUTHOR INFORMATION

Corresponding Author

*E-mail: benice@sc.edu.

ORCID

Julia Pribyl: 0000-0002-9854-2849
Brian Benicewicz: 0000-0003-4130-1232
Andrew Jimenez: 0000-0001-7696-9705
Sanat Kumar: 0000-0002-6690-2221

Notes

The authors declare no competing financial interest.

■ ACKNOWLEDGMENTS

This work was supported by the grant DE-SC0018135 funded by the U.S. Department of Energy, Office of Science. Thank you to Taylor A. Jenkins for help obtaining the Nb-*g*-SiO_2 DLS result.

■ REFERENCES

(1) *PlasticsEurope Annual Review 2017−2018*; PlasticsEurope: Brussels, 2018; https://www.plasticseurope.org/en/resources/publications/498-plasticseurope-annual-review-2017-2018%20European%20polymer%20report (accessed September 10, 2018).

(2) Dorigato, A.; Pegoretti, A. (Re)Processing Effects on Linear Low-Density Polyethylene/Silica Nanocomposites. *J. Polym. Res.* **2013**, *20*, 92.

(3) Nowlin, T. E.; Mink, R. I.; Kissin, Y. V. Supported Magnesium/Titanium-Based Ziegler Catalysts for Production of Polyethylene. In *Handbook of Transition Metal Polymerization Catalysts*, online ed.; Hoff, R., Mather, R. T., Eds.; John Wiley & Sons: Hoboken, NJ, 2010; p 131.

(4) Eisch, J. J. Fifty Years of Ziegler-Natta Polymerization: From Serendipity to Science. A Personal Account. *Organometallics* **2012**, *31*, 4917−4932.

(5) Yang, H.; Huang, B.; Fu, Z.; Fan, Z. Ethylene/1-Hexene Copolymerization with Supported Ziegler-Natta Catalysts Prepared

DOI: 10.1021/acsmacrolett.8b00956
ACS Macro Lett. 2019, 8, 228−232

by Immobilizing $TiCl_3(OAr)$ onto $MgCl_2$. *J. Appl. Polym. Sci.* **2015**, *132*, 41329.
(6) Fu, T.; Liu, Z.; Cheng, R.; He, X.; Tian, Z.; Liu, B. Ethylene Polymerization over $MgCl_2$/ SiO_2 Bi-suppored Ziegler-Natta Hybrid Titanium/Vanadium Catalysts. *Macromol. Chem. Phys.* **2017**, *218*, 1700027.
(7) Yadav, Y. S.; Jain, P. C. Melting Behavior of Isotactic Polypropylene Isothermally Crystallized from the Melt. *Polymer* **1986**, *27*, 721−727.
(8) Bassett, D. C.; Olley, R. H. On the Lamellar Morphology of Isotactic Polypropylene Spherulites. *Polymer* **1984**, *25*, 935−946.
(9) Akcora, P.; Liu, H.; Kumar, S. K.; Moll, J.; Li, Y.; Benicewicz, B. C.; Schadler, L. S.; Acehan, D.; Panagiotopoulos, A. Z.; Pryamitsyn, V.; Ganesan, V.; Ilavsky, J.; Thiyagarajan, P.; Colby, R. H.; Douglas, J. F. Anisotropic Self-Assembly of Spherical Polymer-Grafted Nanoparticles. *Nat. Mater.* **2009**, *8*, 354−359.
(10) Natarajan, B.; Neely, T.; Rungta, A.; Benicewicz, B.; Schadler, L. S. Thermomechanical Properties of Bimodal Brush Modified Nanoparticle Composites. *Macromolecules* **2013**, *46*, 4909−4918.
(11) Bell, M.; Krentz, T.; Nelson, J. K.; Schadler, L.; Wu, K.; Breneman, C.; Zhao, S.; Hillborg, H.; Benicewicz, B. Investigation of Dielectric Breakdown Strength in Silica-Epoxy Nanocomposites using Designed Interfaces. *J. Colloid Interface Sci.* **2017**, *495*, 130−139.
(12) Du, Z.; Zhang, W.; Zhang, C.; Jing, Z.; Li, H. A Novel Polyethylene/Palygorskite Nanocomposite Prepared via In-Situ Coordinated Polymerization. *Polym. Bull.* **2002**, *49*, 151−158.
(13) He, F.-A.; Zhang, L.-M.; Jiang, H.-L.; Chen, L.-S.; Wu, Q.; Wang, H.-H. A New Strategy to Prepare Polyethylene Nanocomposites by Using a Late-Transition Metal Catalyst Supported on $AlEt_3$-Activated Organoclay. *Compos. Sci. Technol.* **2007**, *67*, 1727−1733.
(14) Zhang, J.; Jiang, D. D.; Wilkie, C. A. Polyethylene and Polypropylene Nanocomposites based on a Three Component Oligomerically-Modified Clay. *Polym. Degrad. Stab.* **2006**, *91*, 641−648.
(15) Scott, S. L.; Peoples, B. C.; Yung, C.; Rojas, R. S.; Khanna, V.; Sano, H.; Suzuki, T.; Shimizu, F. Highly Dispersed Clay-Polyolefin Nanocomposites Free of Compatibilizers via the In Situ Polymerization of α-Olefins by Clay-Supported Catalysts. *Chem. Commun.* **2008**, *0*, 4186−4188.
(16) Bergman, J. S.; Chen, H.; Giannelis, E. P.; Thomas, M. G.; Coates, G. W. Synthesis and Characterization of Polyolefin−Silicate Nanocomposites: A Catalyst Intercalation and In Situ Polymerization Approach. *Chem. Commun.* **1999**, 2179−2180.
(17) Ray, S.; Galgali, G.; Lele, A.; Sivaram, S. In Situ Polymerization of Ethylene with Bis(Imino)Pyridine Iron(II) Catalyst Supported on Clay: The Synthesis and Characterization of Polyethylene-Clay Nanocomposites. *J. Polym. Sci., Part A: Polym. Chem.* **2005**, *43*, 304−318.
(18) Kuila, T.; Bose, S.; Mishra, A. K.; Khanra, P.; Kim, N. H.; Lee, J. H. Effect of Functionalized Graphene on the Physical Properties of Linear Low Density Polyethylene Nanocomposites. *Polym. Test.* **2012**, *31*, 31−38.
(19) Ferreira, F. V.; Franceschi, W.; Menezes, B. R. C.; Brito, F. S.; Lozano, K.; Coutinho, A. R.; Cividanes, L. S.; Thim, G. P. Dodecylamine Functionalization of Carbon Nanotubes to Improve Dispersion, Thermal and Mechanical Properties of Polyethylene-Based Nanocomposites. *Appl. Surf. Sci.* **2017**, *410*, 267−277.
(20) Dong, J.-Y.; Liu, Y. Synthesis of Polypropylene Nanocomposites using Graphite Oxide-Intercalated Ziegler-Natta Catalyst. *J. Organomet. Chem.* **2015**, *798*, 311−316.
(21) Virtanen, S.; Krentz, T. M.; Nelson, J. K.; Schadler, L. S.; Bell, M.; Benicewicz, B. C.; Hillborg, H.; Zhao, S. Dielectric Breakdown Strength of Epoxy Bimodal Polymer Brush Grafted Core Functionalized Silica Nanocomposites. *IEEE Trans. Dielectr. Electr. Insul.* **2014**, *21*, 563−570.
(22) Khani, M. M.; Abbas, Z. M.; Benicewicz, B. C. Well-Defined Polyisoprene-Grafted Silica Nanoparticles via the RAFT Process. *J. Polym. Sci., Part A: Polym. Chem.* **2017**, *55*, 1493−1501.
(23) Huang, Y.; Zheng, Y.; Sarkar, A.; Xu, Y.; Stefik, M.; Benicewicz, B. Matrix-Free Polymer Nanocomposite Thermoplastic Elastomers. *Macromolecules* **2017**, *50*, 4742−4753.
(24) Monteil, V.; Stumbaum, J.; Thomann, R.; Mecking, S. Silica/Polyethylene Nanocomposite Particles from Catalytic Emulsion Polymerization. *Macromolecules* **2006**, *39*, 2056−2062.
(25) Toyonaga, M.; Chammingkwan, P.; Terano, M.; Taniike, T. Well-Defined Polypropylene/Polypropylene-Grafted Silica Nanocomposites: Roles of Number and Molecular Weight of Grafted Chains on Mechanistic Reinforcement. *Polymers* **2016**, *8*, 300.
(26) Bieligmeyer, M.; Taheri, S. M.; German, I.; Boisson, C.; Probst, C.; Milius, W.; Altstadt, V.; Breu, J.; Schmidt, H.-W.; D'Agosto, F.; Forster, S. Completely Miscible Polyethylene Nanocomposites. *J. Am. Chem. Soc.* **2012**, *134*, 18157−18160.
(27) Sertchook, H.; Elimelech, H.; Makarov, C.; Khalfin, R.; Cohen, Y.; Shuster, M.; Babonneau, F.; Avnir, D. Composite Particles of Polyethylene@Silica. *J. Am. Chem. Soc.* **2007**, *129*, 98−108.
(28) Khani, M. M.; Woo, D.; Mumpower, E. L.; Benicewicz, B. C. Poly(Alkyl Methacrylate)-Grafted Silica Nanoparticles in Polyethylene Nanocomposites. *Polymer* **2017**, *109*, 339−348.
(29) Zhao, D.; Gimenez-Pinto, V.; Jimenez, A. M.; Zhao, L.; Jestin, J.; Kumar, S. K.; Kuei, B.; Gomez, E. D.; Prasad, A. S.; Schadler, L. S.; Khani, M. M.; Benicewicz, B. C. Tunable Multiscale Nanoparticle Ordering by Polymer Crystallization. *ACS Cent. Sci.* **2017**, *3*, 751−758.
(30) Cao, E.; Pichavant, L.; Prouzet, E.; Heroguez, V. The Formation and Study of Poly(Ethylene Oxide)-Poly(Norbornene) Block-Copolymers on the Surface of Titanium Dioxide Particles: a Novel Approach towards Application of SI-ROMP to Larger Surface Modification. *Polym. Chem.* **2016**, *7*, 2751−2758.
(31) Kalluru, S. H.; Cochran, E. W. Synthesis of Polyolefin/Layered Silicate Nanocomposites via Surface-Initiated Ring-Opening Metathesis Polymerization. *Macromolecules* **2013**, *46*, 9324−9332.
(32) Feng, J.; Stoddart, S. S.; Weerakoon, K. A.; Chen, W. An Efficient Approach to Surface-Initiated Ring-Opening Metathesis Polymerization of Cyclooctadiene. *Langmuir* **2007**, *23*, 1004−1006.
(33) Liu, C.; Kubo, K.; Wang, E.; Han, K.-S.; Yang, F.; Chen, G.; Escobedo, F. A.; Coates, G. W.; Chen, P. Single Polymer Growth Dynamics. *Science* **2017**, *358*, 352−355.
(34) Haque, H. A.; Kakehi, S.; Hara, M.; Nagano, S.; Seki, T. High-Density Liquid Crystalline Azobenzene Polymer Brush attained by Surface-Initiated Ring-Opening Metathesis Polymerization. *Langmuir* **2013**, *29*, 7571−7575.
(35) Alonso-Villanueva, J.; Rodriguez, M.; Vilas, J. L.; Laza, J. M.; Leon, L. M. Ring-Opening Metathesis Polymerization Kinetics of Cyclooctene with Second Generation Grubbs Catalyst. *J. Macromol. Sci., Part A: Pure Appl.Chem.* **2010**, *47*, 1130−1134.
(36) Ganewatta, M. S.; Ding, W.; Rahman, M. A.; Yuan, L.; Wang, Z.; Hamidi, N.; Robertson, M. L.; Tang, C. Bioboased Plastics and Elastomers from Renewable Rosin via "Living" Ring-Opening Metathesis Polymerization. *Macromolecules* **2016**, *49*, 7155−7164.

DOI: 10.1021/acsmacrolett.8b00956
ACS Macro Lett. 2019, 8, 228−232